pISSN 2384-1095
eISSN 2384-1109

iMRI 2016;20:53-60

http://dx.doi.org/10.13104/imri.2016.20.1.53

iMRI
Investigative Magnetic Resonance Imaging

Alternating Acquisition Technique for Quantification of *in vitro* Hyperpolarized [1-^{13}C] Pyruvate Metabolism

Seungwook Yang[1], Joonsung Lee[2], Eunhae Joe[1], Hansol Lee[1], Ho-Taek Song[3], Dong-Hyun Kim[1]

[1]Department of Electrical and Electronic Engineering, Yonsei University, Seoul, Korea
[2]Center for Neuroscience Imaging Research, Institute for Basic Science, Sungkyunkwan University, Suwon, Korea
[3]Department of Radiology, College of Medicine, Yonsei University, Seoul, Korea

Technical Note

Received: February 3, 2016
Revised: March 22, 2016
Accepted: March 22, 2016

Correspondence to:
Dong-Hyun Kim, Ph.D.
Department of Electrical and Electronic Engineering, Room C228, Engineering Hall 3, Yonsei University, 50 Yonsei-ro, Seodaemun-gu, Seoul 03722, Korea.
Tel. +82-2-2123-5874
Fax. +82-2-313-2879
Email: donghyunkim@yonsei.ac.kr

Purpose: To develop a technique for quantifying the ^{13}C-metabolites by performing frequency-selective hyperpolarized ^{13}C magnetic resonance spectroscopy (MRS) *in vitro* which combines simple spectrally-selective excitation with spectrally interleaved acquisition.

Methods: Numerical simulations were performed with varying noise level and K_p values to compare the quantification accuracies of the proposed and the conventional methods. For *in vitro* experiments, a spectrally-selective excitation scheme was enabled by narrow-band radiofrequency (RF) excitation pulse implemented into a free-induction decay chemical shift imaging (FIDCSI) sequence. Experiments with LDH / NADH enzyme mixture were performed to validate the effectiveness of the proposed acquisition method. Also, a modified two-site exchange model was formulated for metabolism kinetics quantification with the proposed method.

Results: From the simulation results, significant increase of the lactate peak signal to noise ratio (PSNR) was observed. Also, the quantified K_p value from the dynamic curves were more accurate in the case of the proposed acquisition method compared to the conventional non-selective excitation scheme. *In vitro* experiment results were in good agreement with the simulation results, also displaying increased PSNR for lactate. Fitting results using the modified two-site exchange model also showed expected results in agreement with the simulations.

Conclusion: A method for accurate quantification of hyperpolarized pyruvate and the downstream product focused on *in vitro* experiment was described. By using a narrow-band RF excitation pulse with alternating acquisition, different resonances were selectively excited with a different flip angle for increased PSNR while the hyperpolarized magnetization of the substrate can be minimally perturbed with a low flip angle. Baseline signals from neighboring resonances can be effectively suppressed to accurately quantify the metabolism kinetics.

Keywords: Hyperpolarized; ^{13}C; Metabolic imaging; *in vitro*; Spectroscopy

INTRODUCTION

Observation of *in vivo* metabolism with ^{1}H magnetic resonance spectroscopy and spectroscopic imaging (MRS, MRSI) can provide detailed information on molecular concentrations of various key neurochemicals such as creatine (1, 2), choline (3, 4), N-acetylaspartic acid (NAA) (5-7) and γ-aminobutyric acid (GABA) (8, 9), and has been applied for diagnosis and observation of treatment responses in patients with various types of cancers. Furthermore, recent advent of dissolution-based dynamic nuclear polarization (DNP) method (10) has allowed spectroscopic acquisition, metabolism quantification and even *in vivo* imaging of metabolites labeled with ^{13}C. Direct spectroscopic examination of metabolic pathways of ^{13}C molecules for both normal and diseased tissues utilizing this new technical breakthrough has shown great clinical potential in the last decade (11-13). Hyperpolarized ^{13}C MRS studies were primarily focused on utilizing lactate dehydrogenase (LDH)-catalyzed ^{13}C label exchange between injected hyperpolarized [1-^{13}C] pyruvate and [1-^{13}C] lactate and also [1-^{13}C] alanine via alanine aminotransferase (14).

Some research also investigated quantifying and modeling these metabolic processes, and has shown that conserving the hyperpolarized magnetization of the substrate and increasing the metabolic product peak signal to noise ratio (PSNR) can potentially benefit accurate kinetic modeling (15-19). This is especially important for *in vitro* experiments since cell number counts are likely to be limited relative to the *in vivo* case. Downstream metabolic products' PSNR can therefore be significantly lower compared to *in vivo* environment, making accurate measurement and quantification of the metabolism kinetics difficult. Also, partly due to low PSNR, signals from the downstream metabolites are likely to be contaminated by neighboring resonances with higher signal, leading to overestimation during quantification process, and it is unclear how much the quantification process is affected.

In this work, an approach for performing *in vitro* hyperpolarized ^{13}C MRS is presented. Experiments with tumor cell aggregate were performed to quantify the cell line's metabolism characteristics regarding LDH-catalyzed ^{13}C label exchange between [1-^{13}C] pyruvate and [1-^{13}C] lactate. To overcome limitations arising from *in vitro* settings, a simple MRS acquisition method which utilizes spectrally-selective excitation radiofrequency (RF) pulse with variable flip angles was developed, which allowed frequency-interleaved acquisition of metabolites in question. Numerical simulations were performed to assess the proposed method's effectiveness in terms of calculating exchange rate constants, and a modified version of the two-site exchange model was formulated for accurate quantification of the acquired data.

METHODS

Modified Two-Site Exchange Model

For quantitative analysis of the acquired data, the two-site exchange model (20) which associates label exchange between two metabolites (i.e., pyruvate and lactate) was modified and used. The model is generally known as follows (21):

$$\text{Pyruvate} \underset{K_L}{\overset{K_P}{\rightleftharpoons}} \text{Lactate} \quad [1]$$

$$dL_z/dt = -\rho_L (L_z - L_\infty) + K_P P_z - K_L L_z \quad [2]$$

$$dP_z/dt = -\rho_P (P_z - P_\infty) + K_L L_z - K_P P_z \quad [3]$$

Where K_P and K_L refers to rate constants by which pyruvate and lactate convert to each other, respectively; L_z and P_z are the z-magnetization of the ^{13}C nucleus in the lactate and pyruvate carboxyl carbons; ρ_L and ρ_P are the spin-lattice relaxation rates ($1/T_{1(L,P)}$); and L_∞ and P_∞ are the equilibrium magnetizations (at $t = \infty$) of lactate and pyruvate. This relationship is true assuming that there is no extra input of the substrate (i.e. [1-^{13}C] pyruvate) and the product (i.e. [1-^{13}C] lactate) from other sites. Here, the effect of excitation flip angles and T_1 relaxation is not considered. Since the proposed method involves spectrally-interleaved acquisition of signals from metabolites at every repetition time (TR) with different flip angles, the 'missing' data for pyruvate and lactate at every TR must be accounted for in Eq. [2-3]. Since the initial ^{13}C-labelled lactate pool is close to zero and the reverse label exchange from ^{13}C lactate to ^{13}C pyruvate will be very small relative to the forward label exchange, Eq. [2] and Eq. [3] can be approximated assuming that the conversion rate from lactate to pyruvate (K_L) is zero. Discretizing the expressions with respect to each TRs, we get:

$$dL_z/dt = \frac{L_z(nTR+TR) - L_z(nTR)}{TR} = \frac{L_z[n+1] - L_z[n]}{TR} \quad [4]$$

$$dP_z/dt = \frac{P_z(nTR+TR)-P_z(nTR)}{TR} = \frac{P_z[n+1]-P_z[n]}{TR} \quad [5]$$

where L_z and P_z represents the magnetization of lactate and pyruvate, TR represents the repetition time, and n refers to the n^{th} TR starting from 1. Then, the modified two-site exchange model can be expressed as follows:

$$L_z[n+1] = (1-\rho_L \cdot TR)\cdot L_z[n]\cdot\cos(\theta_L[n]) + K_P \cdot TR \cdot P_z[n]\cdot\cos(\theta_P[n]) \quad [6]$$

$$P_z[n+1] = (1-\rho_P \cdot TR - K_P \cdot TR)\cdot P_z[n]\cdot\cos(\theta_P[n]) \quad [7]$$

Here, θ_L and θ_P represent excitation flip angles for lactate and pyruvate, respectively. Rewriting Eq. [6] and Eq. [7] and dividing them into odd and even TRs:

$$P_z[2n] = (1-\rho_P \cdot TR - K_P \cdot TR)\cdot P_z[2n-1]\cdot\cos(\theta_P[2n-1]) \quad [8]$$

$$P_z[2n+1] = (1-\rho_P \cdot TR - K_P \cdot TR)\cdot P_z[2n] \quad [9]$$

$$L_z[2n] = (1-\rho_L \cdot TR)\cdot L_z[2n-1] + K_P \cdot TR \cdot P_z[2n-1]\cdot\cos(\theta_P[2n-1]) \quad [10]$$

$$L_z[2n+1] = (1-\rho_L \cdot TR)\cdot L_z[2n]\cdot\cos(\theta_L[2n]) + K_P \cdot TR \cdot P_z[2n] \quad [11]$$

Now using Eq. [8] to Eq. [11], the unmeasured data and the constants K_P, K_L, and ρ can be iteratively estimated.

Simulations

Simulations were performed to compare the quantification accuracies of the proposed alternating acquisition method and conventional non-selective, constant flip angle excitation scheme. Two acquisition methods were compared over varying noise levels and K_P values, while using 1° and 20° flip angles for pyruvate and lactate in the proposed method, and using constant 5° flip angle for the non-selective case. Dynamic curves of pyruvate and lactate were simulated using the modified Bloch equation, then K_P values from each cases were calculated. Then the results were compared to the true value. All numerical simulations and data analysis were done using MATLAB 2014a (Mathworks, Natick, MA, USA).

Excitation RF and MR Pulse Sequence

To enable spectrally-selective excitation, a narrow-band excitation RF pulse was designed using finite impulse response (FIR) filter design method (22). The required spectral bandwidth of the excitation RF pulse was determined from ^{13}C spectra obtained from previous *in vitro* studies conducted under similar 3T environment. Typical peak resonances of [1-^{13}C] pyruvate and its metabolic products showed approximate linewidth of 15 Hz at FWHM, which required the RF passband to be wider than 15 Hz. Also, because the proximity of [1-^{13}C] lactate and [1-^{13}C] pyruvate-hydrate peaks ($\Delta f \approx 120$ Hz) prevents accurate measurement and quantification of converted lactate due to pyruvate-hydrate baseline, the RF stopband was designed to be less than 100 Hz to ensure selective excitation. The FWHM of the designed RF pulse resulted in ≈ 120 Hz with duration of 20.0 ms.

Next, the narrow-band RF excitation pulse was implemented into a free-induction decay chemical shift imaging (FIDCSI) sequence as shown in Figure 1. Since the implemented excitation RF pulse has narrow passband, spectrally-selective excitation was achieved via interleaving the transmit frequency of the RF excitation pulse between [1-^{13}C] pyruvate and [1-^{13}C] lactate resonances at every TRs. Also, by varying the flip angle between the two resonances,

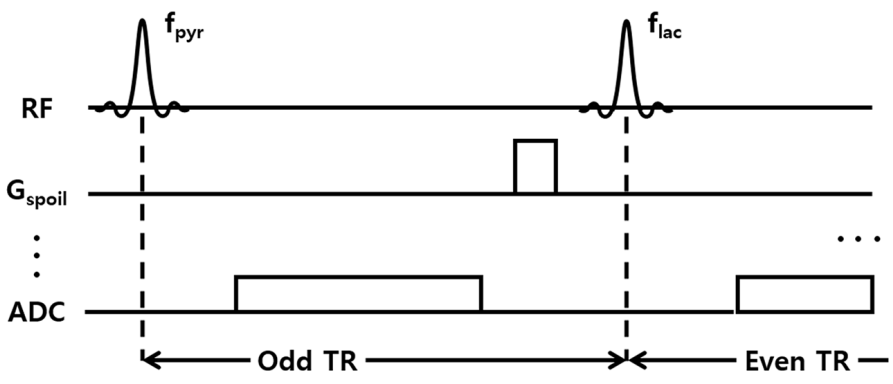

Fig. 1. Simplified pulse sequence diagram for the proposed alternating acquisition mode. Narrow-band frequency-selective excitation RF pulses were implemented into a conventional free-induction decay chemical shift imaging (FID-CSI) sequence to allow spectrally-selective excitation and acquisition of lactate and pyruvate between every TR in an interleaved manner.

relatively low SNR of product lactate was compensated. Flip angles were alternated between 1° for pyruvate and 20° for lactate.

For *in vitro* application of the proposed method, [1-^{13}C] pyruvic acid (Cambridge Isotope, Tewksbury, MA, USA) doped with 15 mM Trityl radical OX-063 (Oxford Instruments, Oxford, UK) and 1.5 mM Dotarem (Guerbet, France) was hyperpolarized using HyperSense DNP polarizer (Oxford Instruments, Oxford, UK). After dissolution into aqueous state, 2.0 mL of the hyperpolarized substrate was injected into the test tube filled with 4.0 mL of LDH (15 U) and 60 uL of NADH (500 mM) solution over 9s. The amount of LDH used for the *in vitro* experiments was determined from separate experiments (data not shown) conducted to recreate typical hyperpolarized [1-^{13}C] spectra obtained in normal *in vivo* cases. The test tube was placed inside the plastic holder structure made as part of the custom-built ^{13}C-tuned solenoid coil prior to the injection. Tubing was placed inside the enzyme mixture and allowed thorough mixing during the substrate injection process. TR of 750 ms was used with 384 repetitions (192 acquisitions each for pyruvate and lactate) over 6.4 minutes of scan time. The procedure was repeated with a constant flip angle scheme using a hard excitation pulse (non-selective excitation) with 5° flip angle for comparison. All experiments were performed on a GE MR750 3T clinical MRI system (GE Healthcare, Waukesha, WI, USA) equipped with a broadband amplifier. The custom-built ^{13}C-tuned solenoid coil was

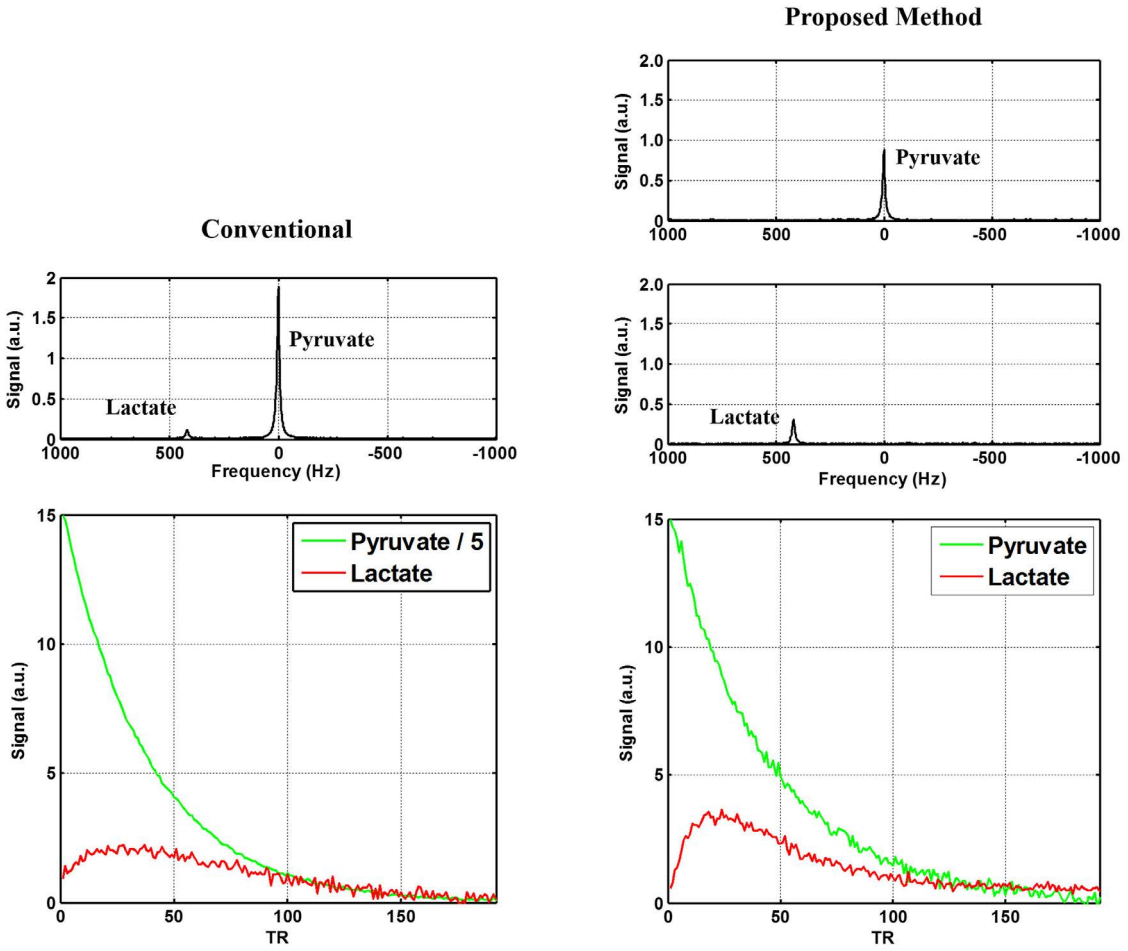

Fig. 2. Simulation results comparing the conventional, non-selective acquisition (a) with the proposed method (b). Time-averaged spectra (top row) show that signal peaks from lactate and pyruvate can be completely separated while also increasing the lactate peak SNR (PSNR) proportional to the flip angle used in the proposed interleaved acquisition scheme. Bottom row displays peak signal dynamics of lactate and pyruvate at every TR.

used for transmission and reception. The temperature of the test tube was maintained at around 36°C using an external heater device for all *in vitro* experiments.

RESULTS

Representative simulated spectra comparing the conventional and the proposed method are shown in Figure 2. Compared to the conventional case (Fig. 2a, top), spectra of pyruvate and lactate using the proposed method are completely separated due to TR-interleaved spectrally-selective acquisition scheme (Fig. 2b, top). The PSNR of lactate is significantly improved in the averaged spectrum, with near 4-fold increase in the peak signal. Pyruvate, on the other hand, shows decreased peak signal level due to lower excitation flip angle. The dynamic curves (Fig. 2, bottom row) indicate that the lactate signal PSNR has generally increased over most TRs, and also that the hyperpolarized magnetization of pyruvate can be slightly prolonged by using the proposed method. The quantified K_p value from the dynamic curve were 0.0018 s^{-1} and 0.000982 s^{-1} for the conventional and proposed method, respectively.

The simulation results show that the proposed method has better performance over most K_P and noise ranges as shown in Figure 3. The estimation error generally increases in both cases for larger K_P values, but the error increased noticeably in the constant case for when the K_P value was small. Both methods displayed similar performance against increasing noise level. Although the noise level is less than 1% of the pyruvate signal, it is still significant since the lactate signal will be at a comparable range with respect to noise. The results are shown as error maps plotted as percent error relative to the input (known) K_P values.

Averaged spectra from dynamic acquisition using conventional FIDCSI sequence and the proposed method is shown in Figure 4 (top row). Enzyme amounts were calibrated so that the resulting spectra would represent cases when cell number count is small. As shown in the conventional case (Fig. 4a), lactate signal is less than 1% of the averaged pyruvate signal. With the proposed method (Fig. 4b), spectra containing pyruvate and lactate are completely separated, with increased lactate signal PSNR. The increased lactate PSNR can be readily observed in the signal dynamic curves as well. Signal from pyruvate, on the other hand, is decreased due to lower excitation flip angle. To avoid transient-state conversion of pyruvate to lactate in the analysis with the two-site exchange model, data fitting was limited to 100 time points after the lactate's peak signal, and the T_1 (ρ^{-1}) of pyruvate and lactate were assumed to be equal (i.e. $\rho_L = \rho_P$ in Eq. [3.8] ~ [3.11]). With the constant flip angle scheme, the proposed fitting method showed ρ of 72.7632 s^{-1} with K_P = 0.0014 s^{-1} and K_L = 0.0176 s^{-1}. With the proposed acquisition method, ρ of 69.2214 s^{-1}

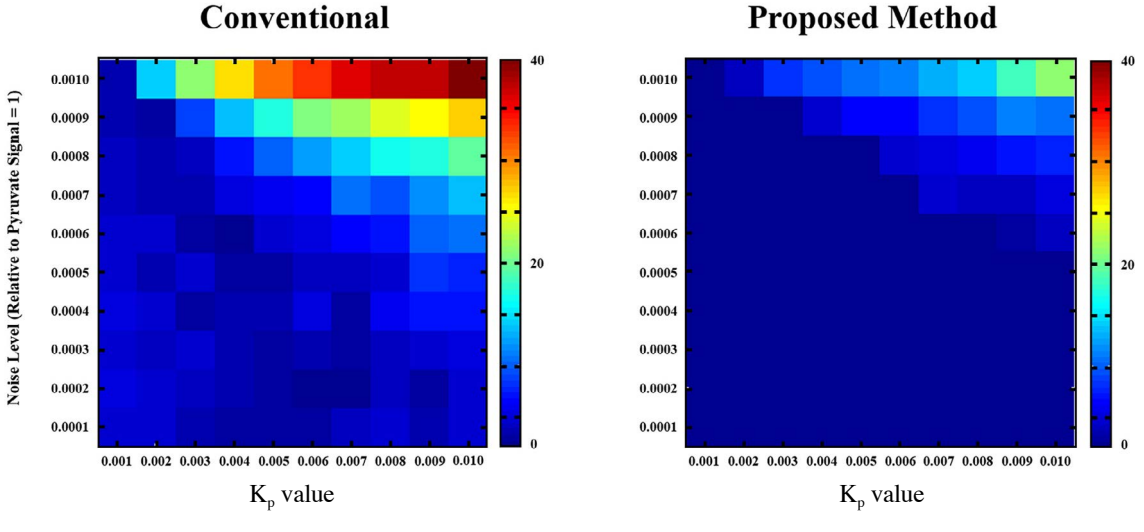

Fig. 3. Comparison of error maps showing estimation error from calculating the apparent conversion rate constant values using the conventional (a) and the proposed method (b). Error values are significantly reduced (maximum error at ~23.0% with the proposed method, down from 40.0% error using the conventional method) over all noise and K_p value ranges.

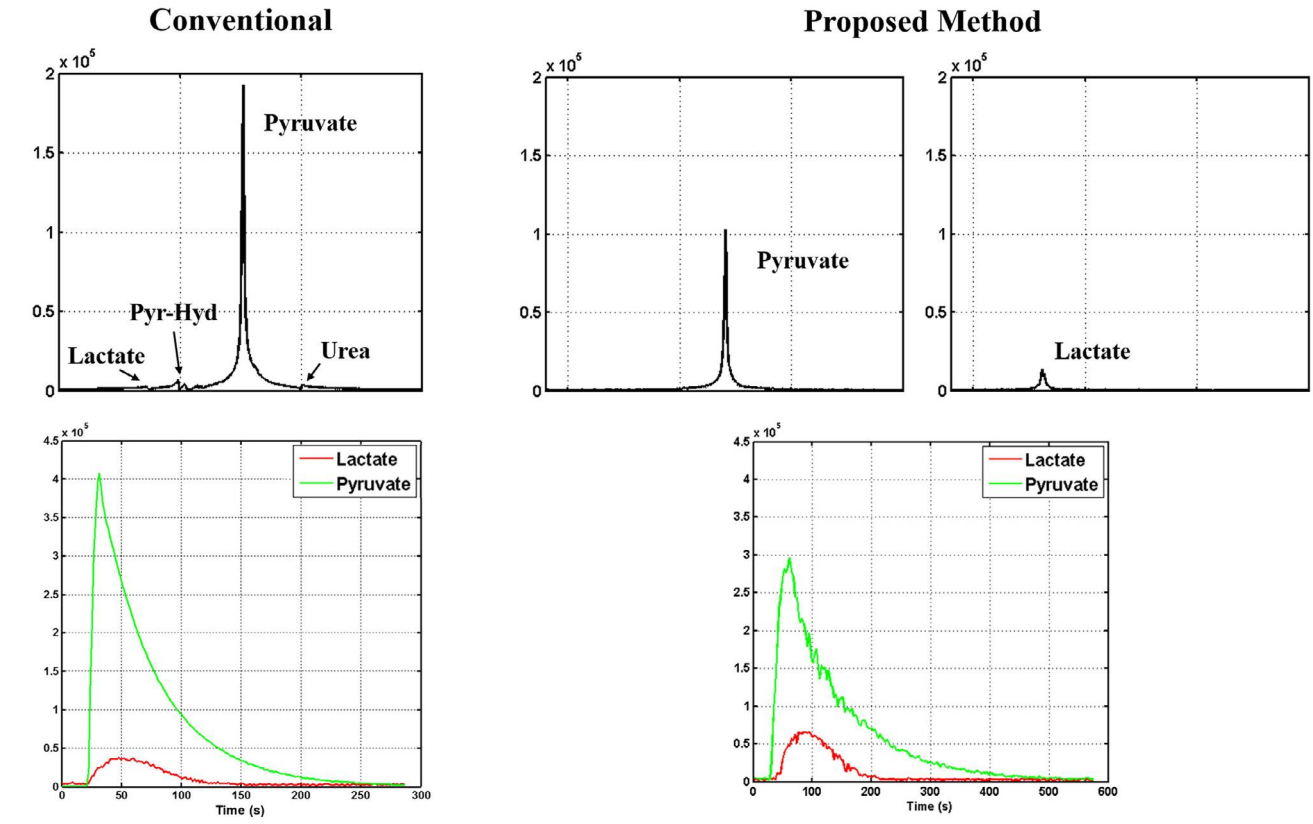

Fig. 4. *In vitro* experiment results comparing the averaged acquired spectra and signal dynamics using the conventional (a) and the proposed method (b). Signals from pyruvate and lactate are completely separated in the case of the proposed method, with increased lactate PSNR.

with $K_P = 0.0024\ s^{-1}$ and $K_L = 0.0162\ s^{-1}$ was obtained.

DISCUSSION AND CONCLUSION

The error maps generated from simulation results show that the error in estimating K_p value can be up to 40% when using the conventional method (Fig. 3a). Over most noise and K_p value ranges, the proposed method seems to be more accurate. Whereas both methods show generally linear increase in the error with respect to increasing true K_p value and noise, it is notable that the error in the conventional case also slightly increased for low K_p and noise. Relating this to the product (lactate) PSNR, it can be said that low product PSNR is the dominating factor of quantification accuracy.

For the *in vitro* experiment, the small difference in the estimated T_1 values could be due to the minor fluctuations in the pyruvate signal (Fig. 4b, bottom) possibly caused by unintended excitation from side-lobe of the 10° flip angle excitation pulses used in the even TR. Side-lobes from the excitation RF pulse could cause unintended excitation of the neighboring resonances such as pyruvate-hydrate or alanine. Although spectral encoding will resolve these signals into different peaks, limitations such as baseline contamination or cases where spectral resolution may not be sufficient could affect the quantification results. To reduce contaminating signals from such resonances, longer excitation RF pulses with narrower passbands and sharper transition bands may be used. However, using long RF pulses is limited by both the T_2* of the metabolites and the FWHM of the resonance peaks. With typical T_2* of ~22 ms (empirically measured, data not shown), long pulse width will compromise the PSNR. Therefore, these factors should be considered during optimal excitation RF pulse design.

Although in this study the exchange rate constants were

calculated from the modified multi-site exchange model, the 'true' value for K_P or K_L is still debatable. As mentioned before, these values are dependent on various conditions such as cell-line characteristics, cellular activeness, delivery and distribution of the substrate/enzymes, etc. Although some of these are controllable during the experiment, dominating biological factors are in many cases beyond control. Another factor which affects the derivation of reaction rate kinetics is the multi-compartment model used. The results frequently become model-dependent and may vary significantly between models, even with same input data. Additionally, the robustness of these model-based approaches can be compromised by the arterial input function (AIF), and also by the chosen signal acquisition window. It was shown that error in AIF could have significant influence in estimating the apparent rate constants from kinetic modeling (23), and some have investigated methods for direct measurement of the AIF (24) or for minimization of its effect on kinetic modeling (25-27). Also, it was shown that the calculated rate constants can vary depending on the signal acquisition timing (28), and that careful determination of optimal acquisition window is necessary for increasing the results' reproducibility. Another group has proposed model-free approach for analyzing the metabolism kinetics which is independent of the AIF or the formulated multi-compartment model (29). However, procuring the downstream products' PSNR is still crucial even for model-free approaches since the dynamic data is still used for the quantification process, which could benefit from the application of the proposed method.

In summary, a method for accurate quantification of hyperpolarized pyruvate and its product lactate focused for *in vitro* hyperpolarized ^{13}C experiments was described. By using a narrow-band excitation RF pulses with alternating transmit frequency at every TR, metabolic product can be selectively excited with a higher flip angle for increased PSNR while the hyperpolarized magnetization of the substrate can be minimally perturbed with a low flip angle. Baseline signals from neighboring resonances can be effectively suppressed to accurately quantify the metabolism kinetics. Furthermore, with the modified version of the two-site exchange model, calculation of the rate constants associated with the conversion was also possible.

Acknowledgments

This research was supported by a grant of the Korea Health Technology R&D Project through the Korea Health Industry Development Institute (KHIDI), funded by the Ministry of Health & Welfare, Republic of Korea (grant number : HI15C2422).

REFERENCES

1. Wallimann T, Wyss M, Brdiczka D, Nicolay K, Eppenberger HM. Intracellular compartmentation, structure and function of creatine kinase isoenzymes in tissues with high and fluctuating energy demands: the 'phosphocreatine circuit' for cellular energy homeostasis. Biochem J 1992;281 (Pt 1): 21-40
2. Saunders DE, Howe FA, van den Boogaart A, Griffiths JR, Brown MM. Aging of the adult human brain: in vivo quantitation of metabolite content with proton magnetic resonance spectroscopy. J Magn Reson Imaging 1999;9:711-716
3. Wang Y, Li SJ. Differentiation of metabolic concentrations between gray matter and white matter of human brain by in vivo 1H magnetic resonance spectroscopy. Magn Reson Med 1998;39:28-33
4. Tan J, Bluml S, Hoang T, Dubowitz D, Mevenkamp G, Ross B. Lack of effect of oral choline supplement on the concentrations of choline metabolites in human brain. Magn Reson Med 1998;39:1005-1010
5. Baslow MH. N-acetylaspartate in the vertebrate brain: metabolism and function. Neurochem Res 2003;28:941-953
6. Birken DL, Oldendorf WH. N-acetyl-L-aspartic acid: a literature review of a compound prominent in 1H-NMR spectroscopic studies of brain. Neurosci Biobehav Rev 1989;13:23-31
7. Clark JB. N-acetyl aspartate: a marker for neuronal loss or mitochondrial dysfunction. Dev Neurosci 1998;20:271-276
8. Brambilla P, Perez J, Barale F, Schettini G, Soares JC. GABAergic dysfunction in mood disorders. Mol Psychiatry 2003;8:721-737, 715
9. Oz G, Terpstra M, Tkac I, et al. Proton MRS of the unilateral substantia nigra in the human brain at 4 tesla: detection of high GABA concentrations. Magn Reson Med 2006;55:296-301
10. Ardenkjaer-Larsen JH, Fridlund B, Gram A, et al. Increase in signal-to-noise ratio of > 10,000 times in liquid-state NMR. Proc Natl Acad Sci U S A 2003;100:10158-10163
11. Nelson SJ, Kurhanewicz J, Vigneron DB, et al. Metabolic imaging of patients with prostate cancer using hyperpolarized [1-(1)(3)C]pyruvate. Sci Transl Med 2013;5:198ra108
12. Park I, Larson PE, Tropp JL, et al. Dynamic hyperpolarized carbon-13 MR metabolic imaging of nonhuman primate

brain. Magn Reson Med 2014;71:19-25
13. Lau AZ, Miller JJ, Robson MD, Tyler DJ. Cardiac perfusion imaging using hyperpolarized (13) c urea using flow sensitizing gradients. Magn Reson Med 2016;75:1474-1483
14. Albers MJ, Bok R, Chen AP, et al. Hyperpolarized ^{13}C lactate, pyruvate, and alanine: noninvasive biomarkers for prostate cancer detection and grading. Cancer Res 2008;68:8607-8615
15. Harrison C, Yang C, Jindal A, et al. Comparison of kinetic models for analysis of pyruvate-to-lactate exchange by hyperpolarized 13 C NMR. NMR Biomed 2012;25:1286-1294
16. Atherton HJ, Schroeder MA, Dodd MS, et al. Validation of the in vivo assessment of pyruvate dehydrogenase activity using hyperpolarised ^{13}C MRS. NMR Biomed 2011;24:201-208
17. Kettunen MI, Hu DE, Witney TH, et al. Magnetization transfer measurements of exchange between hyperpolarized [1-^{13}C] pyruvate and [1-13C]lactate in a murine lymphoma. Magn Reson Med 2010;63:872-880
18. Xu T, Mayer D, Gu M, et al. Quantification of in vivo metabolic kinetics of hyperpolarized pyruvate in rat kidneys using dynamic 13C MRSI. NMR Biomed 2011;24:997-1005
19. Yen YF, Le Roux P, Mayer D, et al. T(2) relaxation times of (13)C metabolites in a rat hepatocellular carcinoma model measured in vivo using (13)C-MRS of hyperpolarized [1-(13)C]pyruvate. NMR Biomed 2010;23:414-423
20. Brindle KM. NMR methods for measuring enzyme kinetics in vivo. Progress in N M R Spectroscopy 1988;20:257-293
21. McConnell HM. Reaction rates by nuclear magnetic resonance. J Chem Phys 1958;28:430-431
22. Oppenheim AV, Willsky AS, Nawab SH. Signals and systems, 2nd ed. Upper Saddle River, NJ: Prentice Hall, 1997:957
23. Kazan SM, Reynolds S, Kennerley A, et al. Kinetic modeling of hyperpolarized (13)C pyruvate metabolism in tumors using a measured arterial input function. Magn Reson Med 2013;70:943-953
24. von Morze C, Larson PE, Hu S, et al. Imaging of blood flow using hyperpolarized [(13)C]urea in preclinical cancer models. J Magn Reson Imaging 2011;33:692-697
25. Zierhut ML, Yen YF, Chen AP, et al. Kinetic modeling of hyperpolarized 13C1-pyruvate metabolism in normal rats and TRAMP mice. J Magn Reson 2010;202:85-92
26. Santarelli MF, Positano V, Giovannetti G, et al. How the signal-to-noise ratio influences hyperpolarized 13C dynamic MRS data fitting and parameter estimation. NMR Biomed 2012;25:925-934
27. Menichetti L, Frijia F, Flori A, et al. Assessment of real-time myocardial uptake and enzymatic conversion of hyperpolarized [1-(1)(3)C]pyruvate in pigs using slice selective magnetic resonance spectroscopy. Contrast Media Mol Imaging 2012;7:85-94
28. Lee H, Lee J, Joe E, et al. Determination of optimal scan time for the measurement of downstream metabolites in hyperpolarized 13C MRSI. Investig Magn Reson Imaging 2015;19:212-217
29. Hill DK, Orton MR, Mariotti E, et al. Model free approach to kinetic analysis of real-time hyperpolarized 13C magnetic resonance spectroscopy data. PLoS One 2013;8:e71996